

Scattering properties of a cylinder fabricated from a left-handed material

Vladimir Kuzmiak* and Alexei A. Maradudin

Department of Physics and Astronomy, University of California, Irvine, California 92697-4575

(Received 30 March 2001; revised manuscript received 22 February 2002; published 31 July 2002)

We study the scattering of an electromagnetic wave from a cylinder of infinite length fabricated from a combined split-ring resonator (SRR) and thin metal wire medium that is characterized by an effective frequency-dependent permittivity $\epsilon_{\text{eff}}(\omega)$ and permeability $\mu_{\text{eff}}(\omega)$ that can both be negative in a certain frequency region, and thus constitutes a left-handed (LH) metamaterial. We evaluate the scattering width of the cylinder in terms of the most general form of the Mie coefficients a_n, b_n that takes into account the magnetic effects through the effective refractive index $n_{\text{eff}}(\omega) = \sqrt{\epsilon_{\text{eff}}(\omega)\mu_{\text{eff}}(\omega)}$. Incident waves of both E polarization (where the electric field is parallel to the axis of the cylinder) and H polarization (where the magnetic field is parallel to the axis of the cylinder) are considered. We find that in the case when the magnetic field is perpendicular to the plane of the SRR, the scattering width as a function of the frequency of the incident wave reveals the resonances of the Mie coefficients a_n and b_n , for both E - and H -polarized incident waves. These peaks occur in the frequency range where the effective refractive index is negative, and they arise from modes that propagate with a negative group velocity. This behavior is consistent with the results of transfer-matrix calculations and transmission experiments on two-dimensional LH metamaterials, which show that the medium becomes transparent to the electromagnetic radiation in this frequency region.

DOI: 10.1103/PhysRevB.66.045116

PACS number(s): 41.20.Jb, 42.25.Bs, 73.20.Mf

I. INTRODUCTION

It has been demonstrated recently, that a substance studied theoretically by Veselago¹ in which the dielectric constant ϵ and the magnetic permeability μ are both negative, can be attained artificially in a metamaterial represented by a periodic medium of split-ring resonators (SRR's) and metallic wires^{2,3} that is characterized by an effective permittivity ϵ_{eff} and permeability μ_{eff} that can both have negative values in a certain frequency range in which the real part of the effective refractive index is negative. By inspecting the Maxwell equations it was shown¹ that if both $\epsilon < 0$ and $\mu < 0$, then \mathbf{E} , \mathbf{H} , and \mathbf{k} form a left-handed set and, thus, the direction of \mathbf{k} is opposite to the direction of the Poynting vector. Consequently, this property gives rise to unusual effects including a reversed Doppler shift, reversed Cerenkov radiation, and an inverse Snell's law. Such materials have been termed left-handed (LH) media.

Up to now both theoretical and experimental efforts²⁻⁷ have focused on the study of the dispersion relations of the thin wire medium that is described by the frequency-dependent dielectric function⁶

$$\epsilon_{\text{eff}}(\omega) = 1 - \frac{\omega_p^2}{\omega^2}. \quad (1.1)$$

Here ω_p is the plasma frequency, which depends on the geometrical parameters of the wires in a manner that allows scaling down ω_p to microwave frequencies. On the other hand, an array of split ring resonators exhibits behavior that can be described by an effective frequency-dependent permeability in the form³

$$\mu_{\text{eff}}(\omega) = 1 - \frac{F\omega^2}{\omega^2 - \omega_0^2 + i\omega\Gamma}. \quad (1.2)$$

As in the case of any new class of materials, especially one with the possibility of technological applications, it is desirable to study as many properties of LH materials as possible. Recently, the scattering of electromagnetic waves from a sphere fabricated from an LH medium was studied in terms of the Mie coefficients that include magnetic effects,⁸ and by evaluating the extinction scattering cross section it was shown how the extinction spectra are affected by the existence of magnetic and plasmon polaritons. Recent experimental achievements in the design of metamaterials that exhibit some of the phenomena predicted in LH media suggest that it is worth exploring the properties of these materials that may lead to interesting and useful applications.

In this paper we investigate the scattering of electromagnetic waves from an infinitely long cylinder fabricated from an LH material. We study separately the effects of the specific forms of the effective permittivity and permeability on the existence of both bulk and surface polaritons, and compare the results to those obtained for a cylinder fabricated from an LH substance. We investigate the scattering properties of such a cylinder by evaluating the total scattering width which, for an infinitely long cylinder, is defined as the scattering cross section per unit length. We distinguish two polarizations of the incident beam. When the electric field is parallel to the axis of the cylinder (E polarization) the scattering width is given by⁹

$$C_s = \frac{4}{k_0} \sum_{n=-\infty}^{\infty} |b_n|^2, \quad (1.3)$$

where

$$b_n = \frac{\sqrt{\epsilon\mu}J_n'(k_i R)J_n(k_0 R) - J_n(k_i R)J_n'(k_0 R)}{J_n(k_i R)H_n'(k_0 R) - \sqrt{\epsilon\mu}J_n'(k_i R)H_n(k_0 R)}, \quad (1.4)$$

$H_n(k_0R) \equiv H_n^{(1)}(k_0R) = J_n(k_0R) + iY_n(k_0R)$ are Hankel functions of the first kind, $J_n(k_0R)$ and $Y_n(k_0R)$ are Bessel functions of the first and second kinds, respectively, and the primes denote differentiation with respect to argument. Here the wave number $k_0 = \omega/c$ represents the propagation constant in vacuum, and the wave number $k_i = \sqrt{\epsilon\mu\omega}/c$ accounts for both electric and magnetic effects in the cylinder.

When the magnetic field is parallel to the axis of the cylinder (H polarization), the scattering width is given by⁹

$$C_s = \frac{4}{k_0} \sum_{-\infty}^{\infty} |a_n|^2, \quad (1.5)$$

where

$$a_n = \frac{\sqrt{\epsilon\mu} J_n(k_i R) J_n'(k_0 R) - J_n'(k_i R) J_n(k_0 R)}{J_n'(k_i R) H_n(k_0 R) - \sqrt{\epsilon\mu} J_n(k_i R) H_n'(k_0 R)}. \quad (1.6)$$

The coefficients b_n and a_n attain maximum values at frequencies that satisfy the equations

$$J_n(k_i R) H_n'(k_0 R) - \sqrt{\epsilon\mu} J_n'(k_i R) H_n(k_0 R) = 0, \quad (1.7)$$

$$J_n'(k_i R) H_n(k_0 R) - \sqrt{\epsilon\mu} J_n(k_i R) H_n'(k_0 R) = 0, \quad (1.8)$$

respectively, which are equivalent to the equations for material E and H polaritons.⁹ To investigate the scattering width of cylinders fabricated from LH materials we employ the effective dielectric function for a thin wire mesh given by Eq. (1.1) and the frequency-dependent permeability that describes a SRR medium given by

$$\mu_{\text{eff}}(\omega) = 1 - \frac{F\omega_0^2}{\omega^2 - \omega_0^2 + i\omega\Gamma}, \quad (1.9)$$

which is the effective permeability given by Eq. (1.2) modified in order to insure that $\mu(\omega) \rightarrow 1$ as $\omega \rightarrow \infty$.

It was shown⁵ that by combining the frequency-dependent permittivity of the fine wire mesh and the effective frequency-dependent permeability for the SRR medium in the absence of dissipation, one obtains in the case that the magnetic field \mathbf{H} is perpendicular to the plane of the SRR (H_{\parallel} polarization) the effective refractive index in the form—see Fig. 1(a)

$$n_{\text{eff}}^{\parallel} = \frac{1}{\omega} \sqrt{\frac{(\omega^2 - \omega_p^2)(\omega^2 - \omega_b^2)}{(\omega^2 - \omega_0^2)}}, \quad (1.10a)$$

where

$$\omega_b = \omega_0 / \sqrt{1 - F}. \quad (1.10b)$$

Then the dispersion relation of the combined medium in the form⁵

$$k^2 = \frac{(\omega^2 - \omega_p^2)}{c^2} \frac{(\omega^2 - \omega_b^2)}{(\omega^2 - \omega_0^2)} \quad (1.10c)$$

leads in the frequency range $\omega_0 < \omega < \omega_b$ to a band with negative group velocity, and thus the wave propagates in the direction opposite to the energy flux.

In the case that the magnetic field \mathbf{H} is parallel to the plane of the SRR (H_{\perp} polarization), the effective refractive index shown in Fig. 1(b) is given by

$$n_{\text{eff}}^{\perp} = \frac{1}{\omega} \sqrt{\frac{(\omega^2 - \omega_p^2)(\omega^2 - \omega_f^2)}{(\omega^2 - \omega_0^2)}}, \quad (1.11a)$$

where

$$\omega_f^2 = \omega_0^2 \omega_p^2 / (\omega_0^2 + \omega_p^2). \quad (1.11b)$$

According to the dispersion relation⁵ of the combined medium in the case of H_{\perp} polarization

$$k^2 = \frac{(\omega^2 - \omega_p^2)}{c^2} \frac{(\omega^2 - \omega_f^2)}{(\omega^2 - \omega_0^2)}, \quad (1.11c)$$

the group velocity of the band in the frequency range $\omega_f < \omega < \omega_0$ is positive. Therefore, in contrast to the case of H_{\parallel} polarization, the direction of the wave propagation is not reversed. This effect can be explained in terms of the strong dispersion in this frequency range, which gives rise to a large value of $dn(\omega)/d\omega$, and as a result the sign of the group velocity given by $v_g = c/[n(\omega) + \omega dn(\omega)/d\omega]$ becomes positive.

II. RESULTS

In order to evaluate the effect of the effective refractive index on the scattering width we consider according to Ref. 5 the following configurations of the electromagnetic wave incident on the combined SRR/metal wire medium: E -polarized wave in the case of H_{\parallel} with electric field parallel to the axis of the cylinder and with the magnetic field perpendicular to the plane of the SRR, E -polarized wave in the case of H_{\perp} (with the electric field parallel to the axis of the cylinder and with the magnetic field parallel to the plane of the SRR), H -polarized wave in the case of H_{\parallel} (with the magnetic field which is parallel to the axis of the cylinder and perpendicular to the plane of the SRR), and H -polarized wave in the case of H_{\perp} (with the magnetic field which is parallel both to the axis of the cylinder and to the plane of the SRR).

It has been established⁵ that the behavior of the split ring medium in the case of the parallel and perpendicular polarizations H_{\parallel}, H_{\perp} is dominated by magnetic and dielectric response, respectively. Namely, a band gap revealed by dispersion relation was found in either case, although in the case of the parallel polarization the gap is interpreted as being due to negative $\mu_{\text{eff}}(\omega)$, while the H_{\perp} gap originates from negative $\epsilon_{\text{eff}}(\omega)$. Taking into account the interpretation of the H_{\parallel} and H_{\perp} gaps for a split ring medium and the effective refractive indices for both polarizations given by Eqs. (1.10a) and (1.11a) we evaluate the scattering width in terms of the coefficients a_n and b_n for the following configurations: split ring medium for the parallel and perpendicular polarization characterized by

$$\mu(\omega) = \mu_{\text{eff}}^{\parallel}(\omega) = \frac{\omega^2 - \omega_b^2}{\omega^2 - \omega_0^2}, \quad \epsilon(\omega) = 1 \quad (2.1)$$

and

$$\mu(\omega) = 1, \quad \epsilon(\omega) = \epsilon_{\text{eff}}^{\perp}(\omega) = \frac{\omega^2 - \omega_f^2}{\omega^2 - \omega_0^2}. \quad (2.2)$$

Then we perform the same calculations for a combined SRR/metal wire medium characterized by effective refractive indices n_{eff}^{\perp} and $n_{\text{eff}}^{\parallel}$ given by Eqs. (1.10a) and (1.11a), respectively, for both E and H polarization of the incident wave. Here we scale $\omega_0, \omega_b, \omega_f$ with respect to the plasma frequency ω_p .

We first study the behavior of H modes for the H_{\parallel} polarization by evaluating the coefficients a_n and the C_s^n components of the scattering width C_s given by Eq. (1.5) for a single cylinder fabricated from a metal characterized by the Drude free-electron model form of the dielectric function given by Eq. (1.1). For the radius $R = 0.5545c/\omega_p$ which for $\omega_p = 12$ GHz yields the value $R = 1.38$ cm, we found the H_{11}^s and H_{21}^s resonances at $\omega_{11}^s/\omega_p = 0.674$ and $\omega_{21}^s/\omega_p = 0.697$, respectively. These resonances correspond to surface modes converging to ω_s from below, where the surface plasmon frequency $\omega_s = \omega_p/\sqrt{2}$ is obtained from $\epsilon(\omega_s) = -1$. Here we label the modes in the form H_{np}^s , where n is the order of the Bessel function in Eq. (1.3), p labels the solutions for given n in the order of increasing magnitude, and the superscript s indicates a surface mode, while bulk modes are not explicitly indicated by a superscript. An analogous notation is used for E modes.

The spectrum of the H modes for a cylinder fabricated from a split ring medium that is characterized by an effective frequency-dependent permeability $\mu_{\text{eff}}^{\parallel}(\omega)$, while $\epsilon_{\text{eff}}(\omega) = 1$ consists of two types of modes resulting from the resonances of the Mie coefficients a_n into which we substitute the permeability given by Eq. (2.1), where $\omega_0 = 0.5$ and $\omega_b = 0.707$. Namely, for the cylinder radius $R = 0.5545c/\omega_p$ we found the H_{01} resonance at $\omega_{01}^H/\omega_p = 0.496$ due to the magnetic bulk polariton, and the H_{11} and H_{21} resonances at $\omega_{11}^H/\omega_p = 0.604$ and $\omega_{21}^H/\omega_p = 0.610$ in the frequency range where $\mu_{\text{eff}}^{\parallel}$ is negative. The H_{11} and H_{21} resonances due to the surface magnetic polaritons converge to ω_s^H from below, where $\omega_s^H = (\omega_0^2 + \omega_b^2)^{1/2}/\sqrt{2}$ is the root of the equation obtained from $\mu_{\text{eff}}^{\parallel}(\omega) = -1$. By using the values $\omega_0 = 0.5$ and $\omega_b = 0.707$ one obtains $\omega_s^H = 0.612$. In Fig. 2(a) we present in addition to the C_s^n components of the total scattering width for H -polarized waves also those found for the cylinder fabricated from a metallic material having $\mu_{\text{eff}} = 1$.

To evaluate the coefficients a_n for a single cylinder fabricated from an LH material in the case of H_{\parallel} polarization we employ the effective refractive index $n_{\text{eff}}^{\parallel}$ given by Eq. (1.10a), where $\omega_0 = 0.5$ and $\omega_b = \omega_p/\sqrt{2}$, which was evaluated by using Eq. (1.10b) with $F = 0.5$. By using these parameters we plot the effective refractive index $n_{\text{eff}}^{\parallel}$ shown in Fig. 1(a), where the lower x axis corresponds to the dimensionless frequency normalized with respect to the plasma fre-

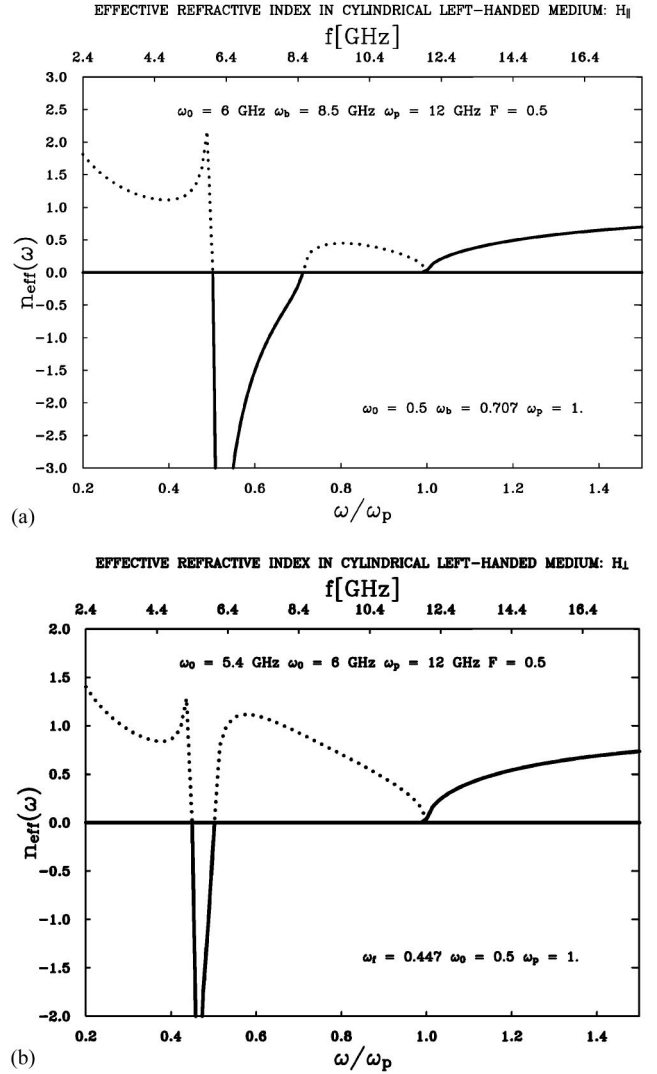


FIG. 1. (a) Effective refractive index $n_{\text{eff}}^{\parallel}(\omega)$ for an LH medium that corresponds to an H -polarized incident wave. Solid and dotted curves indicate the real and imaginary branches of $n_{\text{eff}}^{\parallel}(\omega)$ versus the dimensionless frequency ω/ω_p (lower x axis) and the experimentally compatible values $\omega_0 = 6$ GHz, $\omega_b = 8.5$ GHz, and $\omega_p = 12$ GHz (upper x axis). (b) Effective refractive index $n_{\text{eff}}^{\perp}(\omega)$ for an LH medium that corresponds to an E -polarized incident wave. Solid and dotted curves indicate the real and imaginary branches of $n_{\text{eff}}^{\perp}(\omega)$ versus the dimensionless frequency ω/ω_p (lower x axis) and the experimentally compatible values $\omega_f = 5.4$ GHz, $\omega_0 = 6$ GHz, and $\omega_p = 12$ GHz (upper x axis), when $F = 0.1$.

quency ω_p , while the upper x axis corresponds to the experimentally compatible values $\omega_0 = 6$ GHz, $\omega_b = 8.5$ GHz, and $\omega_p = 12$ GHz. The solid curve indicates the real part of the refractive index, which is negative when both the permittivity and permeability are negative, while the dotted curve corresponds to the imaginary part of the refractive index.

No resonances were found for frequencies below ω_0 and in the range $\omega_0 < \omega < \omega_b$ in which dispersion is characterized by a positive, pure imaginary, effective refractive index, while we found H_{01} , H_{11} , and H_{21} resonances due to the

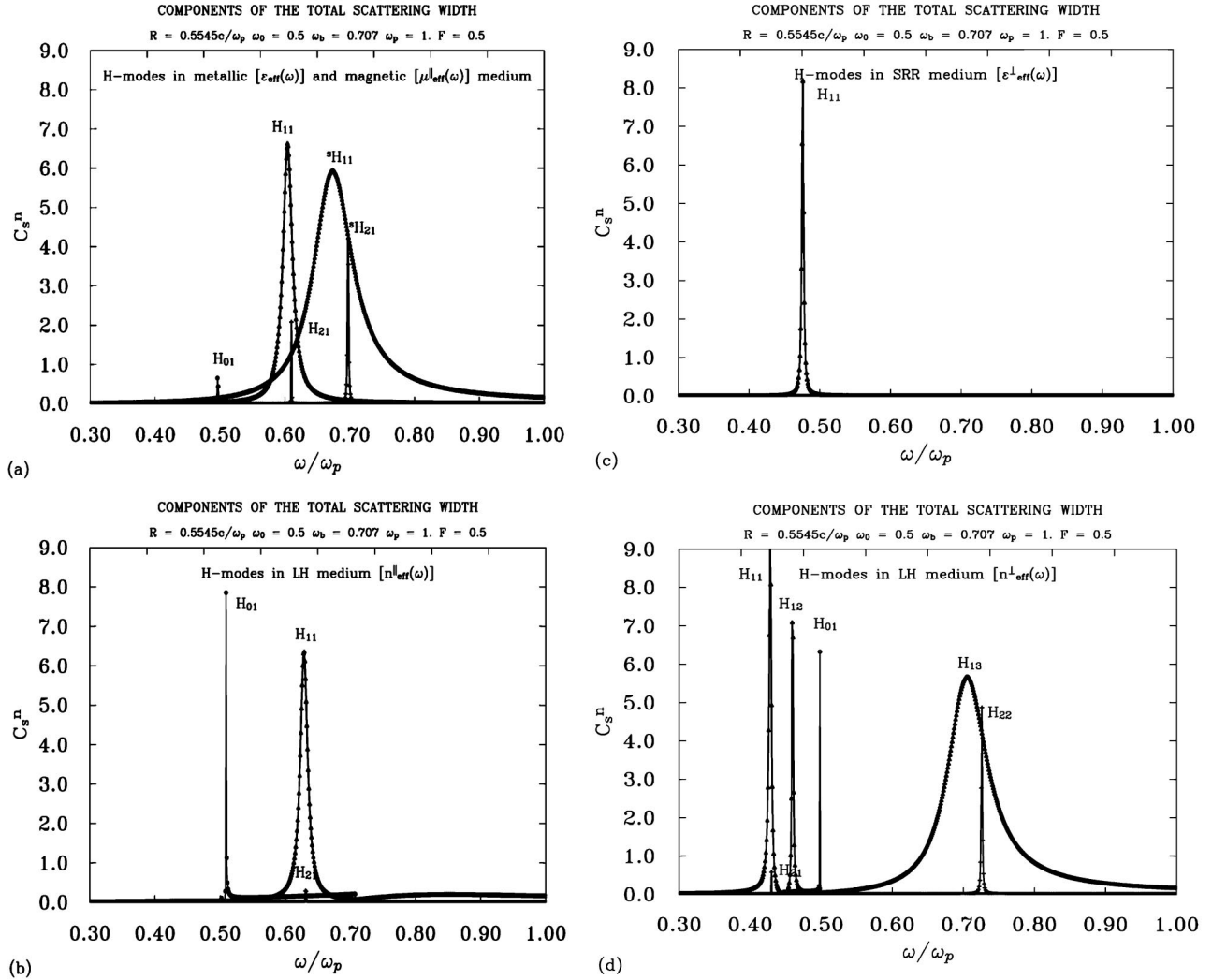


FIG. 2. (a) The C_s^n components of the total scattering width for H polarization that correspond to the H_{01} and H_{11} resonances associated with a cylinder fabricated from a medium characterized by the frequency-dependent permeability $\mu_{\text{eff}}^{\parallel}(\omega)$ given by Eq. (2.1), where $\omega_0 = 0.5$ and $\omega_b = 0.707$ compared to the ${}^sH_{11}$ and ${}^sH_{21}$ surface modes associated with a metallic cylinder characterized by a free-electron effective refractive index. (b) The C_s^n components of the total scattering width for H polarization that correspond to the H_{01} , H_{11} , and H_{21} resonances due to the surface and bulk polaritons found in a cylinder fabricated from an LH material characterized by $n_{\text{eff}}^{\parallel}(\omega)$ shown in Fig. 1(a). (c) The spectrum of H modes for H_{\perp} that consists of the H_{11} resonance associated with a cylinder fabricated from a split ring medium characterized by the frequency-dependent permittivity $\epsilon_{\text{eff}}^{\perp}(\omega)$ given by Eq. (2.2), where $\omega_f = 0.4472$ and $\omega_0 = 0.5$, while $F = 0.5$. (d) The C_s^n components of the total scattering width for H polarization that correspond to the H_{11} , H_{21} , H_{12} , H_{01} , H_{13} , and H_{22} resonances due to the surface and bulk polaritons found in a cylinder fabricated from an LH material characterized by $n_{\text{eff}}^{\parallel}(\omega)$ shown in Fig. 1(b).

bulk polaritons shown in Fig. 2(b) at $\omega_{01}^H/\omega_p = 0.509$, $\omega_{11}^H/\omega_p = 0.629$, and $\omega_{21}^H/\omega_p = 0.631$, respectively.

Now we consider behavior of a split ring and a combined SRR/metal wire medium in the case of H_{\perp} polarization. The spectrum of the H -modes for a cylinder fabricated from a medium that is characterized by an effective frequency-dependent permittivity $\epsilon_{\text{eff}}^{\perp}(\omega)$ given by Eq. (2.2) reveals for the cylinder radius $R = 0.5545c/\omega_p$ an H_{01} resonance at $\omega_{01}^H/\omega_p = 0.503$ due to a surface plasmon polariton—see Fig. 2(c).

To study the behavior of an LH cylinder in the case of H_{\perp} polarization we employed the effective refractive index n_{eff}^{\perp} given by Eq. (1.11a) in evaluating the coefficients a_n , for

$\omega_f = 0.447$ and $\omega_b = \omega_p/\sqrt{2}$. We depict the effective refractive index n_{eff}^{\perp} with these parameters in Fig. 1(b), where the lower x axis corresponds to the dimensionless frequency ω/ω_p , while the upper x axis corresponds to the experimentally compatible values $\omega_f = 5.4$ GHz, $\omega_0 = 6$ GHz, and $\omega_p = 12$ GHz. The solid and dotted curves indicate the real and imaginary parts of the refractive index, respectively. For a cylinder fabricated from an LH material in the case of H_{\perp} polarization we found two types of peaks, namely, H_{11} , H_{21} resonances at $\omega_{11}^H/\omega_p = 0.428$, and $\omega_{21}^H/\omega_p = 0.430$, respectively, an H_{12} resonance at $\omega_{12}^H/\omega_p = 0.459$, and H_{13} , H_{22} resonances at $\omega_{13}^H/\omega_p = 0.705$, $\omega_{22}^H/\omega_p = 0.726$, respectively, which are due to surface polaritons—see Fig. 2(d). In addition,

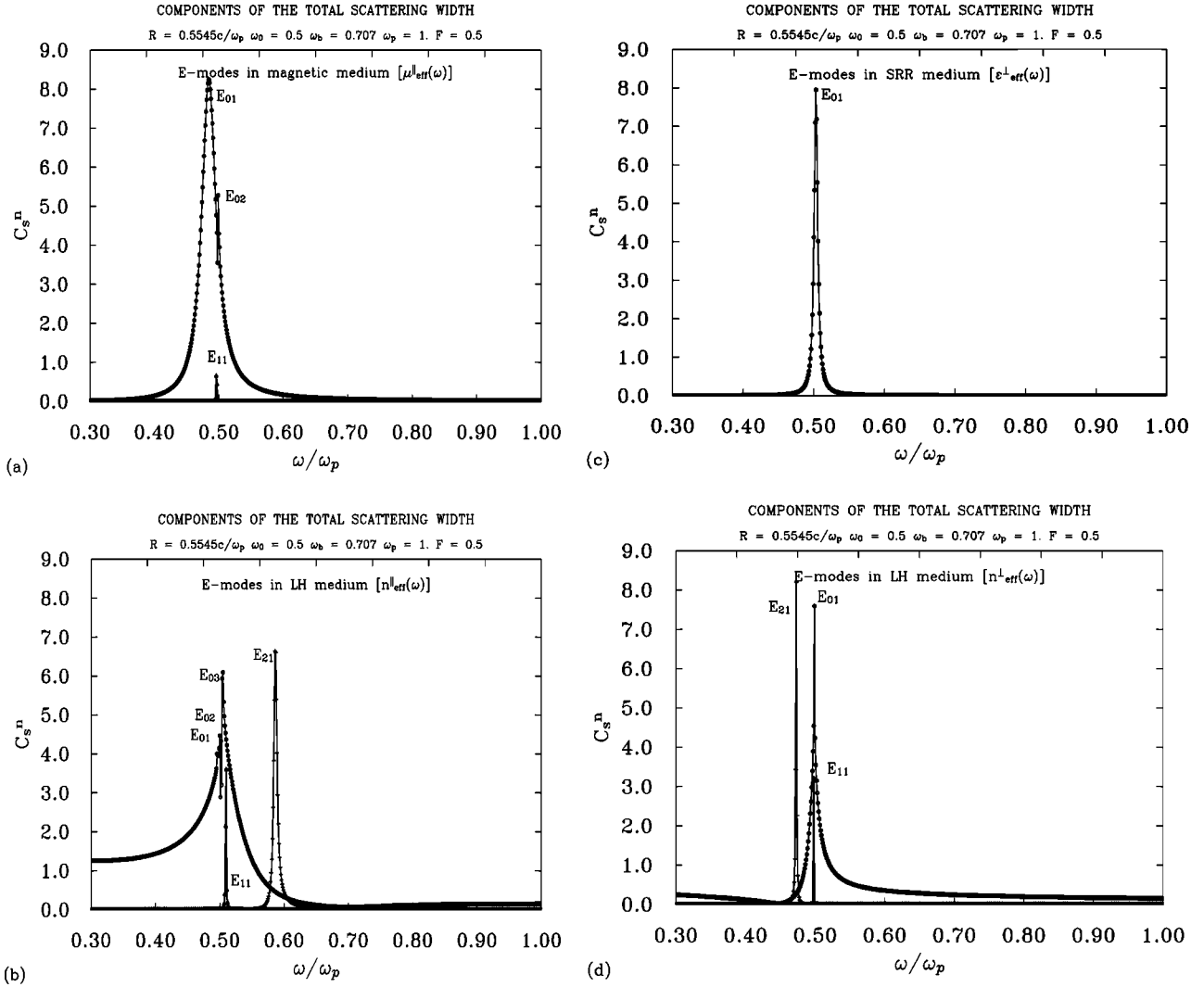


FIG. 3. (a) The C_s^n components of the total scattering width for E polarization that correspond to the magnetic bulk polaritons E_{01} , E_{11} , and E_{02} associated with a cylinder fabricated from a split ring medium characterized by the frequency-dependent permeability $\mu_{\text{eff}}^{\parallel}(\omega)$ given by Eq. (2.1). (b) The C_s^n components of the total scattering width for E polarization associated with the E_{01} , E_{02} , E_{03} , E_{11} , and E_{21} resonances [found in a cylinder fabricated from an LH material characterized by $n_{\text{eff}}^{\parallel}(\omega)$ shown in Fig. 1(b)] that correspond to bulk polaritons. (c) The spectrum of E modes for H_{\parallel} that consists of the E_{01} resonance associated with a cylinder fabricated from a split ring medium characterized by the frequency-dependent permittivity $\epsilon_{\text{eff}}^{\perp}(\omega)$ given by Eq. (2.2). (d) The C_s^n components of the total scattering width for E polarization associated with the E_{21} , E_{11} , and E_{01} resonances found in a cylinder fabricated from an LH material characterized by the $n_{\text{eff}}^{\perp}(\omega)$ shown in Fig. 1(b) that correspond to bulk polaritons.

tion we found a peak H_{01} due to a bulk polariton at $\omega_{01}^H/\omega_p = 0.498$.

Next we proceed to the case of E -polarized electromagnetic waves incident on both an SRR and an LH medium for both parallel and perpendicular polarization of the magnetic field \mathbf{H} to the plane of the SRR, by evaluating the coefficients b_n and the C_s^n components of the scattering width C_s given by Eq. (1.3). It has already been established¹⁰ that there are no E modes in the frequency range below ω_p in the case of the metallic cylinder. Figure 3(a) shows that the spectrum of E modes for a cylinder fabricated from a split ring medium that is characterized by frequency-dependent permeability $\mu_{\text{eff}}^{\parallel}(\omega)$ reveals only peaks below ω_0 , namely, the E_{01} , E_{11} , and E_{02} resonances at $\omega_{01}^E/\omega_p = 0.485$, $\omega_{11}^E/\omega_p = 0.485$, and $\omega_{02}^E/\omega_p = 0.499$ due to magnetic bulk polaritons.

For a cylinder fabricated from an LH medium that is characterized by an effective refractive index $n_{\text{eff}}^{\perp}(\omega)$ given by Eq. (1.11a) we found for E -polarized modes the E_{01} resonance at $\omega_{11}^E/\omega_p = 0.4496$ and the E_{02} , E_{03} , E_{11} , and E_{21} resonances at $\omega_{02}^E/\omega_p = 0.502$, $\omega_{03}^E/\omega_p = 0.505$, $\omega_{11}^E/\omega_p = 0.510$, and $\omega_{21}^E/\omega_p = 0.586$, respectively, all of which are due to bulk polaritons—see Fig. 3(b).

To explore E modes supported by a cylinder fabricated from a split ring medium with an effective frequency-dependent permittivity $\epsilon_{\text{eff}}^{\perp}(\omega)$ given by Eq. (2.2), where $\omega_f = 0.4472$ and $\omega_0 = 0.5$, we evaluate the coefficients b_n given by Eq. (1.4). For the cylinder radius $R = 0.5545c/\omega_p$ we found the E_{01} resonance at $\omega_{01}^E/\omega_p = 0.503$ due to a bulk plasmon polariton, while no E modes below ω_f and within the frequency range $\omega_f < \omega < \omega_0$ were found. The existence

of this resonance is demonstrated in Fig. 3(c) in terms of the C_s^n components of the total scattering width for an E -polarized wave when the magnetic field \mathbf{H} is perpendicular to the plane of the SRR.

For a cylinder fabricated from an LH medium that is characterized by a frequency-dependent permeability $n_{\text{eff}}^\perp(\omega)$ given by Eq. (1.11a) no resonances were found in the frequency regions $\omega < \omega_f$ and $\omega_0 < \omega < \omega_p$ where the effective refractive index attains positive imaginary values, while we found the E_{21} resonance at $\omega_{21}/\omega_p = 0.473$ due to the surface polariton which converges to ω_s^E from below, where $\omega_s^E = (\omega_0^2 + \omega_f^2)^{1/2}/\sqrt{2}$ is the root of the equation obtained from $\mu_{\text{eff}}^\perp(\omega_s^E) = -1$. By using the values $\omega_0 = 0.447$ and $\omega_0 = 0.5$ one obtains $\omega_s^E = 0.474$. In addition, we have found in the frequency range $\omega_f < \omega < \omega_0$ the E_{11} and E_{01} resonances at $\omega_{11}^E/\omega_p = 0.498$, and $\omega_{01}^E/\omega_p = 0.499$, respectively, which correspond to bulk modes. The existence of these modes is documented in Fig. 3(b), where we show the components C_s^n of the total scattering width when the magnetic field \mathbf{H} is perpendicular to the plane of the SRR.

As we have shown previously, the spectrum of metallic cylinders in the case of H polarization consists of peaks that are due to surface plasmon polaritons. These peaks result from the resonances of the Mie coefficients a_n , and they appear in the frequency range where the refractive index is imaginary. The frequencies at which the resonances occur depend on the radius of the cylinder. Therefore, the peaks are expected to appear also in a left-handed medium when the positions of the resonances occur in the frequency region where the refractive index is imaginary. We indeed observed these H modes, namely, H_{13} and H_{22} shown in Fig. 2(d) for the case of H_\perp polarization in the frequency range $\omega_0 < \omega < \omega_p$. On the other hand, they have not been found in the case of H_\parallel polarization. The flexibility inherent to metamaterials gives us the possibility to control the frequency regions with profoundly different behavior of the refractive index, as is demonstrated in Figs. 1(a)–1(b). By varying the geometrical parameters that enter the expressions given by Eqs (1.1) and (1.2) it is possible to design the effective refractive indices in ways that support (or restrict) the existence of the modes corresponding to the resonances of the Mie coefficients. Specifically, in the case of ϵ_{eff} the general form of the plasma frequency is $\omega_p = (d^2L/4\pi)^{-1/2}$, where L is the self-inductance per unit length and d is a wire radius.² For the effective permeability the variation can be achieved by changing the fractional area of the unit cell occupied by the interior of the split ring $F = \pi r^2/a^2$, where a is the lattice constant and r is the inner radius of the split ring.^{2,3}

To demonstrate the idea of controlling of the existence of the modes we modify n_{eff}^\parallel by setting $\omega_0/\omega_p = 0.9$ and using Eq. (1.10b) to obtain $\omega_b/\omega_p = 0.95$, when $F = 0.102$. We employ both modified expressions for n_{eff}^\parallel in the evaluation of the a_n coefficients. We found for the cylinder radius $R = 0.5545c/\omega_p$ the H_{11}, H_{21}, H_{22} , and H_{12} resonances which are due to surface polaritons at $\omega_{11}^H/\omega_p = 0.719, \omega_{21}^H/\omega_p = 0.751, \omega_{22}^H/\omega_p = 0.881$, and $\omega_{12}^H/\omega_p = 0.885$, respectively. In the frequency region $\omega_0 < \omega < \omega_b$, where n_{eff}^\parallel is negative, we also found the H_{01} and H_{13} resonances due to bulk polaritons

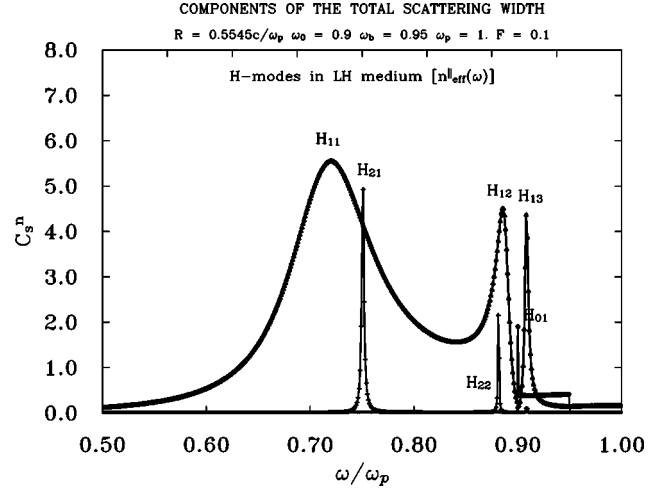


FIG. 4. The C_s^n components of the total scattering width for H polarization that correspond to the bulk polaritons H_{11}, H_{21}, H_{22} , and H_{12} that lie below ω_0 . The H_{01} and H_{13} resonances occur in the frequency range $\omega_0 < \omega < \omega_b$. The cylinder is characterized by a modified effective refractive index $n_{\text{eff}}^\parallel(\omega)$ with $\omega_0/\omega_p = 0.9$ and $\omega_b/\omega_p = 0.95$, when $F = 0.102$ and $R = 0.5545c/\omega_p$.

at $\omega_{01}^H/\omega_p = 0.9001$ and $\omega_{13}^H/\omega_p = 0.908$, respectively. The C_s^n components of the total scattering width associated with these resonances are shown in Fig. 4.

III. DISCUSSION AND CONCLUSION

To summarize the properties of a cylinder characterized by a frequency-dependent permittivity and a frequency-dependent permeability, in comparison with the case where the electric and magnetic contributions are present separately, we start from the spectrum for a metallic cylinder characterized by a frequency-dependent dielectric function of the form (1.1) which consists of peaks due to H -type surface plasmon polaritons [H_{11}^s, H_{21}^s —see Fig. 2(a)] which occur in the frequency range below the plasma frequency ω_p , where the dielectric function is negative. The existence of these modes has been discussed previously,¹⁰ and it has been suggested that they give rise to nearly dispersionless flat bands observed in the photonic band structure for H -polarized electromagnetic wave propagating through a 2D photonic crystal consisting of metallic cylinders.

The spectrum of cylinders fabricated from a lossless split ring medium characterized by an effective permeability and permittivity of the form (2.1) and (2.2) for H_\parallel and H_\perp polarizations reveals two types of peaks for H modes, namely, those in the frequency ranges $\omega_0 < \omega < \omega_b$ [H_{11}, H_{21} —see Fig. 2(a)] for H_\parallel , and $\omega_f < \omega < \omega_0$ [H_{11} —see Fig. 2(c)] for H_\perp , due to surface magnetic and plasmon polaritons, respectively. In addition, we found a peak below ω_p for H_\parallel [H_{01} —see Fig. 2(a)] that is due to a bulk magnetic polariton. In the case of an E -polarized electromagnetic wave the spectrum of the cylinder fabricated from SRR medium reveals peaks only below ω_0 [E_{01}, E_{02} , and E_{11} —see Fig. 3(a)] for H_\parallel , and only above ω_0 [E_{01} —see Fig. 3(c)] for H_\perp , which are due to bulk magnetic and plasmon polaritons, respectively.

It is interesting to note that peaks found for H and E modes in a SRR medium for both H_{\parallel} and H_{\perp} polarizations resemble qualitatively the behavior observed in the case of an isolated cylinder fabricated from GaAs,¹¹ where we found that below the transverse optical mode frequency ω_T there exist both E - and H -bulk modes, while within the polariton gap $\omega_T < \omega < \omega_L$, where $\omega_T(\omega_L)$ is the transverse (longitudinal) optical mode frequency, only surface H modes are supported.

The scattering properties of a cylinder having both a dispersive permittivity and a dispersive permeability are of central interest, in particular in the frequency range where both characteristics are negative, which corresponds to the case when cylinder exhibits the behavior of a left-handed medium. For H_{\parallel} and H_{\perp} polarizations we found H modes [H_{01}, H_{11} , and H_{21} —see Fig. 2(b)] and E modes [E_{02}, E_{03} , and E_{11} —see Fig. 3(b)] in the frequency range $\omega_0 < \omega < \omega_b$, which correspond to bulk polaritons. These peaks indicate the existence of propagating modes with a negative group velocity. Such a behavior is consistent with the results of transfer-matrix calculations and transmission experiments for the case of H_{\parallel} polarization in two-dimensional left-handed metamaterials,^{5,7} according to which the medium becomes transparent in this frequency range.

In the case of H_{\perp} polarization we found for H modes both surface and bulk modes [H_{12}, H_{01} —see Fig. 2(d)] in the frequency range $\omega_f < \omega < \omega_0$, while only bulk modes are sup-

ported in this frequency range for an E -polarized EM wave. It is worth pointing out that the direction of the propagating modes in the frequency range $\omega_f < \omega < \omega_0$ is not reversed with respect to the energy flux, in contrast to the H_{\parallel} polarization. In addition to modes within the frequency region $\omega_f < \omega < \omega_0$, in H_{\parallel} polarization the radiation can excite surface H modes below and above this region [H_{11}, H_{21}, H_{13} , and H_{22} —see Fig. 2(d)] and bulk E modes below ω_f .

Finally, we have demonstrated that by choosing suitable combinations of the geometrical parameters characterizing a combined SRR/metal wire medium it is possible to design the effective refractive indices $n_{\text{eff}}^{\parallel}$ and n_{eff}^{\perp} in such a way that the peaks due to surface polaritons occur in the frequency range where the effective refractive index becomes imaginary for both parallel and perpendicular polarizations of the magnetic field to the plane of the SRR, and thus we can design metamaterials in which incident electromagnetic radiation excites surface polaritons irrespective of the polarization. This result may be interesting for applications based on the surface excitations.

ACKNOWLEDGMENTS

The research was supported by in part by NSF Grant No. INT-932651.

*Permanent Address: Institute of Radio Engineering and Electronics, Czech Academy of Sciences, Chaberska 57, 182 51 Prague 8, Czech Republic.

¹V.G. Veselago, Sov. Phys. Usp. **10**, 509 (1968).

²J.B. Pendry, A.J. Holden, W.J. Stewart, and I. Youngs, Phys. Rev. Lett. **76**, 4773 (1996).

³J.B. Pendry, A.J. Holden, D.J. Robbins, and W.J. Stewart, IEEE Trans. Microwave Theory Tech. **47**, 2075 (1999).

⁴D.R. Smith, D.C. Vier, W. Padilla, S.C. Nemat-Nasser, and S. Schultz, Appl. Phys. Lett. **75**, 1425 (1999).

⁵D.R. Smith, W. Padilla, D.C. Vier, S.C. Nemat-Nasser, and S.

Schultz, Phys. Rev. Lett. **84**, 4184 (2000).

⁶D.R. Smith and N. Kroll, Phys. Rev. Lett. **85**, 2933 (2000).

⁷R.A. Shelby, D.R. Smith, S.C. Nemat-Nasser, and S. Schultz, Appl. Phys. Lett. **78**, 489 (2000).

⁸R. Ruppin, Solid State Commun. **116**, 411 (2000).

⁹R. Englman and R. Ruppin, J. Phys. C **1**, 1515 (1968).

¹⁰V. Kuzmiak, A.A. Maradudin, and F. Pincemin, Phys. Rev. B **50**, 16 835 (1994).

¹¹V. Kuzmiak, A.A. Maradudin, and A.R. McGurn, Phys. Rev. B **55**, 4298 (1997).